



Worm-like mesoporous structured iron-based fluoride: Facile preparation and application as cathodes for rechargeable lithium ion batteries



Yan Lu, Zhaoyin Wen*, Kun Rui, Xiangwei Wu, Yanming Cui

CAS Key Laboratory of Materials for Energy Conversion, Shanghai Institute of Ceramics, Chinese Academy of Sciences, 1295 Ding Xi Road, Shanghai 200050, PR China

HIGHLIGHTS

- An environmental-friendly method to fabricate $\text{Fe}_{1.9}\text{F}_{4.75}\cdot0.95\text{H}_2\text{O}$ is developed.
- The morphology of $\text{Fe}_{1.9}\text{F}_{4.75}\cdot0.95\text{H}_2\text{O}$ is controllable.
- Ionic liquid plays essential multifunctional roles in fabricating the materials.
- The one with worm-like mesoporous structure shows promising cathode performances.

ARTICLE INFO

Article history:

Received 8 October 2012

Received in revised form

27 December 2012

Accepted 5 January 2013

Available online 12 January 2013

Keywords:

Rechargeable lithium ion batteries

Iron-based fluoride

Cathode

Ionic liquid

Mesoporous structure

ABSTRACT

A worm-like mesoporous structured iron-based fluoride ($\text{Fe}_{1.9}\text{F}_{4.75}\cdot0.95\text{H}_2\text{O}$) is successfully synthesized for the first time by a rapid microwave irradiation heating route using ionic liquid 1-butyl-3-methylimidazolium tetrafluoroborate (BmimBF_4) as fluorine source and iron (III) nitrate nonahydrate ($\text{Fe}(\text{NO}_3)_3\cdot9\text{H}_2\text{O}$) as iron source. By controlling the amount of ionic liquid, a series of nanostructured iron-based fluoride materials with different morphologies are obtained. A possible formation mechanism related to the role of the ionic liquid is proposed. The electrochemical performances of the worm-like mesoporous structured iron-based fluoride as cathodes for rechargeable lithium batteries are investigated. A high discharge plateau around 2.7 V at the first cycle, a reversible discharge capacity as high as 145 mAh g^{-1} at a current density of 14 mA g^{-1} and a good rate performance with a high rate capacity of 125 mAh g^{-1} even at 71 mA g^{-1} are obtained.

© 2013 Elsevier B.V. All rights reserved.

1. Introduction

In comparison with the most extensively investigated sulfides and oxides used as cathode materials in lithium batteries in recent years, fluorides attract considerable attention for energy conversion and storage due to the high electronegativity of fluorine [1–3]. Among them, iron-based fluoride with high electromotive force (emf) and theoretical capacity as well as low material cost shows great potential as cathode of rechargeable lithium batteries [4–7]. But the use of erosive and toxic fluoride sources (such as HF) in the synthesis process limits its application to a great extent [8]. Therefore, environmentally friendly and operationally safe fluoride sources are in an urgent need to develop. Several groups have been

devoted to the fabrication and formation mechanism of nanostructured iron-based fluoride using ionic liquid containing fluoride ions as fluoride source [8–10]. David and his coworkers prepared nanostructured FeF_2 successfully using 1-butyl-3-methylimidazolium tetrafluoroborate (BmimBF_4) as fluoride source by a microwave heating method [10]. And the morphology of the prepared nanostructured FeF_2 was tuned by the addition of different amount of water. But the electrochemical properties of these materials were rarely given. Recently, Li and his coworkers reported two nanostructured iron-based fluoride cathode materials (orthorhombic $\text{FeF}_3\cdot0.33\text{H}_2\text{O}$ and cubic $\text{Fe}_{1.9}\text{F}_{4.75}\cdot0.95\text{H}_2\text{O}$) fabricated using BmimBF_4 as fluoride source, whose capacities of 154 mAh g^{-1} and 90 mAh g^{-1} at the current density of 14 mA g^{-1} were obtained respectively. What's more, a systematic study in the formation mechanism of these iron-based fluorides was made and the results showed that BmimBF_4 played an essential role in the formation of the nanostructured iron-based fluorides because it

* Corresponding author. Tel.: +86 21 52411704; fax: +86 21 5241 3903.

E-mail address: zywen@mail.sic.ac.cn (Z. Wen).

served as not only a fluorine source but also a co-solvent and soft template [8]. Considering the advantages of ionic liquid in synthesizing nanostructured iron-based fluorides, as well as its disadvantage of high cost, to investigate the effect of the amount of ionic liquid on the morphology of nanostructured iron-based fluorides is necessary. Besides, it is believed that the investigation would also help us to make a better understand about the mechanism of the formation of iron-based fluoride and provide the basis for fabricating the optimal nanostructured fluoride electrode materials.

Among the various reported synthesis methods of fluoride materials [6–8], the microwave-assisted synthesis is considered to be a promising method. Since its first reports in 1986 [16,17], the applications of microwave heating in synthetic chemistry and materials preparation have been a fast growing area of research [11]. The biggest advantage of the microwave-assisted synthesis lies in its rapid volumetric heating process, providing rapid and uniform heating of reagents, solvents, intermediates, and products, resulting in higher reaction rate, time saving, low energy consumption and higher efficiency compared with conventional heating methods, benefiting the formation of monodispersed small nanostructures [18]. Especially when the ionic liquid is involved in the reaction system, its high polarity resulted from the presence of large organic positive ions makes itself an excellent media for absorbing microwaves, thus leading to a very high heating rate. Recently, a variety of nanostructured materials with controllable morphologies have been synthesized by combining the advantages of both room temperature ionic liquid and microwave heating [19,20].

Herein, a worm-like mesoporous structured iron-based fluoride ($\text{Fe}_{1.9}\text{F}_{4.75} \cdot 0.95\text{H}_2\text{O}$) has been successfully synthesized for the first time using ionic liquid (BmimBF_4) as fluorine source and $\text{Fe}(\text{NO}_3)_3 \cdot 9\text{H}_2\text{O}$ as iron source by a rapid microwave irradiation heating route. By controlling the amount of ionic liquid, a series of nanostructured iron-based fluoride materials with different morphologies are fabricated, indicating the role of the ionic liquid played in the preparation process. A possible mechanism for the formation of the particular nanostructured fluorides is proposed. The obtained materials have been unambiguously characterized using X-ray diffraction (XRD), transmission electron microscopy (TEM), scanning electron microscopy (SEM) and BET measurement. The results show that all of the prepared materials have a structure of cubic $\text{Fe}_{1.9}\text{F}_{4.75} \cdot 0.95\text{H}_2\text{O}$ and the morphologies of them can be tuned by changing the amount of ionic liquid while keeping the other conditions unchanged. Electrochemical performances of the prepared $\text{Fe}_{1.9}\text{F}_{4.75} \cdot 0.95\text{H}_2\text{O}$ material with a worm-like mesoporous structure as the cathode for rechargeable lithium battery are also examined. A reversible discharge capacity as high as 145 mAh g^{-1} at the current density of 14 mA g^{-1} and a high rate capacity of 125 mAh g^{-1} even at 71 mA g^{-1} are obtained.

2. Experimental

2.1. Material preparation

Iron-based fluorides with various morphologies were synthesized using ionic liquid 1-butyl-3-methylimidazolium tetrafluoroborate (BmimBF_4) (Shanghai Cheng Jie Chemical Co. Ltd., 99%) as fluorine source and iron (III) nitrate nonahydrate $\text{Fe}(\text{NO}_3)_3 \cdot 9\text{H}_2\text{O}$ as iron source (Sinopharm Chemical Reagent Co., Ltd.) through a microwave irradiation heating method. Specifically, given amounts of BmimBF_4 ionic liquid (1 mL, 3 mL, 5 mL, 10 mL) were mixed with the fixed amount of metal nitrate salts (1 g) in ethyl alcohol solvent (10 mL) respectively with rigorous stirring for 1 h. Then the mixtures were heated in a microwave oven (MDS-6,

Sino, Shanghai, China) to 80°C rapidly and kept under this condition for 5 min. After completion of the reaction, the products were washed six times with acetone and ethanol to remove the ionic liquid and other organic impurities followed by centrifugation for 10 min at 10,000 rpm. The washed products were dried under vacuum at 60°C and used for further investigation.

2.2. Material characterization

The phases of the prepared materials were checked by X-ray powder diffraction using a Rigaku Ultima IV (40 kV/30 mA) with $\text{Cu-K}\alpha$ radiation. Scanning electron microscopy (SEM, S-4800N, Hitachi) and transmission electron microscopy (TEM, JEM-2100F) were further used to characterize the morphology and structure of the products. The specific surface area was measured by the Brunauer–Emmett–Teller (BET) method using nitrogen adsorption–desorption isotherms on a Micromeritics Tristar 3000 analyzer, and the pore size distribution was obtained from the desorption branch of the isotherm by the Barrett–Joyner–Halenda (BJH) method.

2.3. Electrochemical measurements

The electrochemical performances of the prepared material as cathode for lithium-ion battery were examined in coin type cells. In a typical process, the working electrodes were prepared by dispersing a blend of the as-obtained active material, acetylene black, and polyvinylidene difluoride (PVDF) at the gravimetric ratio of 80:10:10 in *N*-methyl-2-pyrrolidone (NMP). The slurry was then cast onto an aluminum foil and dried in vacuum at 80°C for 2 days. Then coin cells were fabricated using high-purity lithium foil (China Energy Lithium Co., Ltd) as the counter electrode and the reference electrode, Celgard 2400 as the separator, and a solution of 1 M LiPF_6 in ethylene carbonate (EC)/dimethyl carbonate (DMC) (1:1, in wt%) as the electrolyte. The assembly of cells was processed in an argon filled glove box with oxygen and water contents less than 1 ppm. The galvanostatic charge/discharge tests were conducted on a LANDCT2001A battery test system in the voltage range of 1.6–4.5 V (versus Li/Li^+) at the current densities of 14 mA g^{-1} and 71 mA g^{-1} respectively. All the electrochemical tests were performed at room temperature and the current density and specific capacity were calculated on the base of the prepared activematerials.

3. Results and discussion

Fig. 1 shows the X-ray diffraction patterns of the prepared iron fluorides. As seen, well-defined XRD peaks assigned to the cubic $\text{Fe}_{1.9}\text{F}_{4.75} \cdot 0.95\text{H}_2\text{O}$ are detected for all of the four samples, demonstrating that the amount of ionic liquid has no effect on the phase of the products. Compared with the iron source, the valence of the iron cation in the products $\text{Fe}_{1.9}\text{F}_{4.75} \cdot 0.95\text{H}_2\text{O}$ is lower, which is considered to be resulted from the reducing characteristic of BmimBF_4 ionic liquid [8].

The changes of the morphology of the prepared materials are characterized by transmission electron microscopy (TEM, **Fig. 2**) and scanning electron microscopy (SEM, **Fig. 3**). From **Fig. 2**, we can see that the morphology of the prepared materials changes a lot with the varying of the amount of ionic liquid. In order to distinguish the obtained materials with different morphologies, the products are designated as F-X (F represents iron-based fluorides and X represents the amount of ionic liquid used in the preparation process). So the samples F-1, F-3, F-5, F-10 represent the obtained iron-based fluorides using BmimBF_4 of 1 mL, 3 mL, 5 mL and 10 mL in their preparation process respectively.

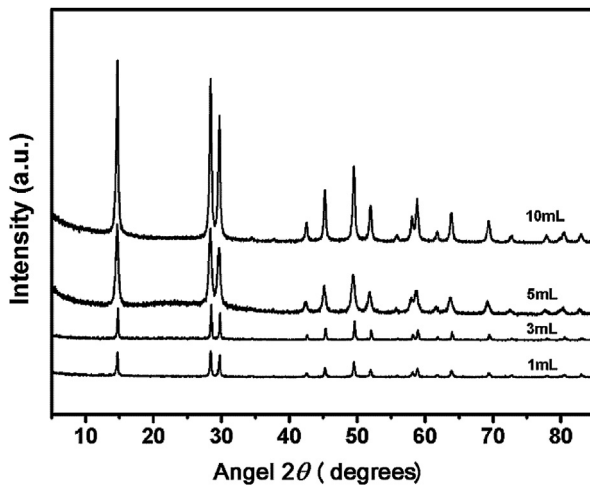


Fig. 1. XRD patterns of the prepared iron-based fluorides.

The details of the changes in the morphology of the prepared materials are further confirmed by SEM images as Fig. 3(a–d) indicated. From Fig. 3(a–d), we can see that with the increase of the amount of ionic liquid from 1 mL to 10 mL, the morphologies of the products show a successive change from nanostructured octahedrons (F-1) to a mixture of nanostructured octahedrons and nanostructured spheres (F-3), to nanostructured spheres (F-5) and

finally nanostructured spheres with worm-like nanopores on the surface (F-10).

It is interesting to see that the nanostructured spheres present in the samples of F-3, F-5 and F-10 are developed from the nanostructured octahedrons present in the sample F-1, which can be unambiguously confirmed from the semi-formed nanostructured sphere as the red circle indicated in Fig. 3(a) and most of the nanostructured spheres in Fig. 3(b). And for Fig. 3(c,d), uniform morphologies of nanostructured spheres are obtained due to the completed growth of nanospheres when the ionic liquid is excess. This phenomena indicates that the morphology of Fe_{1.9}F_{4.75}·0.95H₂O synthesized by a microwave-assisted heating method is controllable by tuning the amount of ionic liquid used in the reaction system.

Moreover, compared with F-1, F-3 and F-5 samples, F-10 sample with worm-like nanopores on the surface of nanostructured spheres is more attractive when used as the cathode for rechargeable lithium battery due to the following two reasons: on one hand, the presence of these worm-like nanopores can increase the specific surface of the materials and enlarge the contact area with the electrolyte; on the other hand, these worm-like nanopores can efficiently accommodate the volume change of the cathode materials during Li⁺ insertion/extraction cycles and thus prevent the pulverization of electrode. What is more, nitrogen adsorption–desorption method is further used to examine the nature of the nanopores of F-10 sample. As Fig. 3(e) indicated, the nitrogen isotherms of F-10 sample is of type IV curve according to the IUPAC classification and featured capillary condensation in the

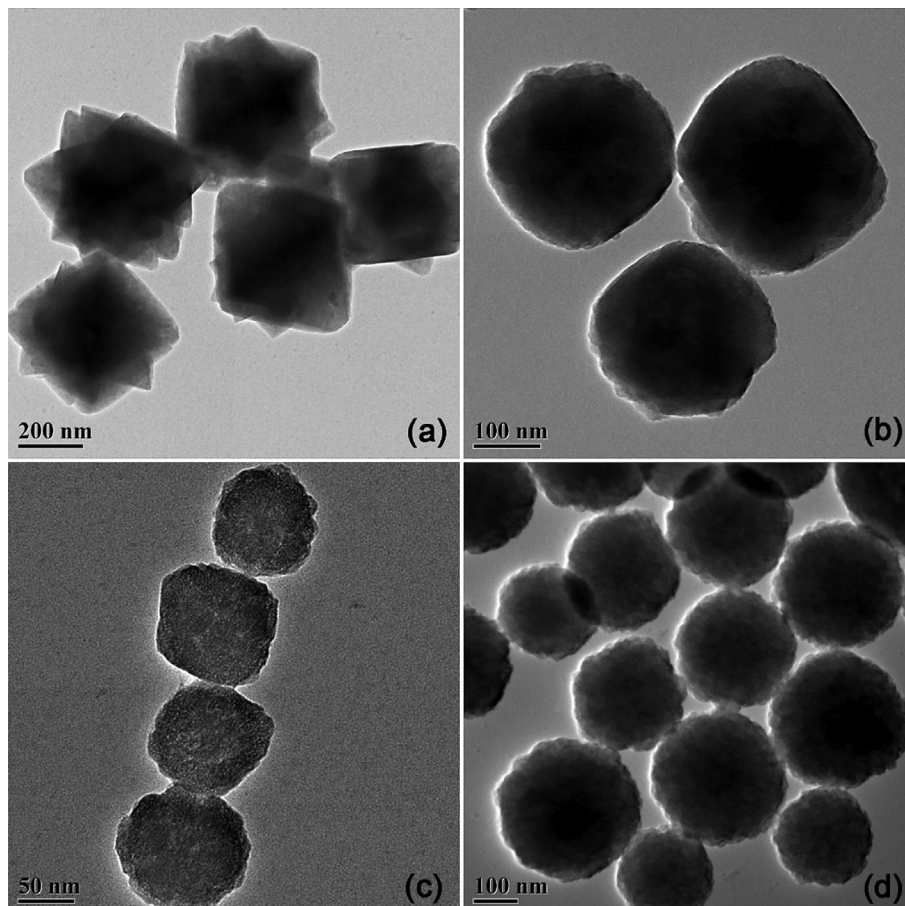


Fig. 2. TEM images of the prepared materials (a. sample F-1, b. sample F-3, c. sample F-5, d. sample F-10).

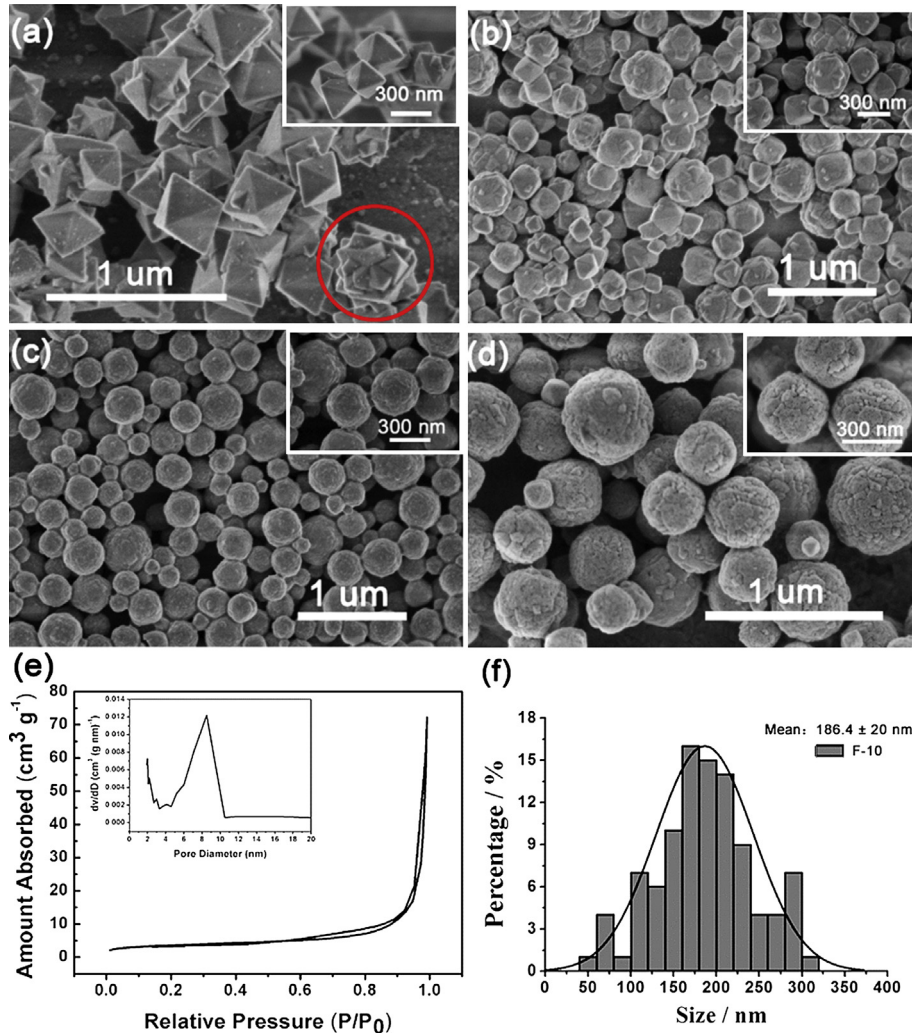


Fig. 3. SEM images of F-1 sample (a), F-3 sample (b), F-5 sample (c) and F-10 sample (d); nitrogen adsorption–desorption isotherms and BJH pore size distributions (e) and diameter distributions (f) of F-10 sample.

mesopores, indicating the presence of mesopores in the prepared material. The mean pore diameter is about 8 nm according to the BJH pore size distribution curve and the BET specific surface is about $13 \text{ m}^2 \text{ g}^{-1}$. And the diameter distribution of F-10 sample is also measured from SEM micrographs using Image J software (NIH, USA), indicating that F-10 has a relatively homogeneous diameter and the average diameter of about (186.4 ± 20) nm (Fig. 3(f)) further proves the nanostructure of F-10 sample. Based on the above analysis, we can see that the prepared F-10 sample has a worm-like mesoporous structure which would be beneficial for its cathode performances for rechargeable lithium batteries.

A possible formation mechanism of the obtained iron-based fluorides with different morphologies is proposed as Fig. 4 depicted. The ionic nature and thermal stability of the BmimBF₄ ionic liquid make itself very good solvent for absorbing microwave radiation [11]. In the microwave frequency range, the ionic liquids with high polarity try to orientate with the electric field. When they try to re-orientate with respect to an alternating electric field, they lose energy in the form of heat by friction [18]. Therefore, the boiling temperature of the mixture solution of BmimBF₄, ethanol and Fe(NO₃)₃·9H₂O can be reached within a very short time. Then the BF₄⁻ anion undergoes fast hydrolysis in the presence of transition metal salts with hydration water molecules (Fe(NO₃)₃·9H₂O) under microwave superheating [12,13] as the following reaction

equation indicated, showing ionic liquid an ideal fluorine source [10,14].



Consequently, solvated Fe³⁺ combines with the F⁻ ion to form precipitated iron based fluorides with nanostructured morphology. By varying the amount of ionic liquid (1 mL, 3 mL, 5 mL, 10 mL) used in the preparation process with other conditions unchanged, we can see that the morphologies of the obtained materials change successively. As demonstrated in Fig. 3(a–d), the nanostructured spheres present in the samples of F-3, F-5 and F-10 are developed from the nanostructured octahedrons present in the sample F-1, which proves that the ionic liquid plays important role in the morphology formation of iron-based fluorides. But the details of the morphology evolution are needed to be further investigated in the future. When the amount of ionic liquid is excessive, a worm-like mesoporous structured iron-based fluoride is formed, which is considered to be ascribed to the template function of the ionic liquids. Through the whole formation process of iron-based fluorides, we can see that ionic liquid plays essential multifunctional roles, including an effective microwave radiation acceptor, a soft template for nanostructure, as well as an environmentally friendly and operationally safe fluoride source. Therefore, we can conclude

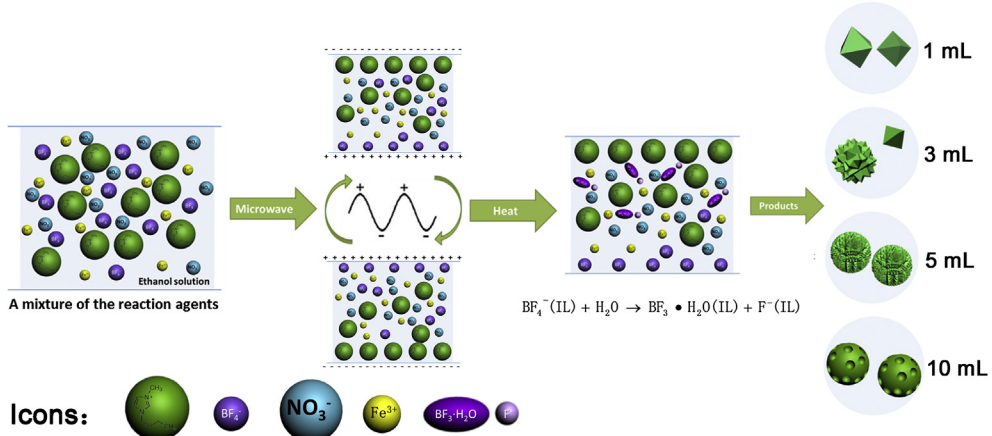


Fig. 4. Scheme of the synthesis mechanism of $\text{Fe}_{1.9}\text{F}_{4.75} \cdot 0.95\text{H}_2\text{O}$ materials with different morphologies.

that the synergy of these functions of ionic liquid contributes to the fabrication of iron-based fluorides with controllable morphologies.

The electrochemical performances of the worm-like mesoporous structured iron-based fluoride as cathodes for rechargeable lithium ion batteries have been investigated. As Fig. 5(a) indicated, two plateaus located at 2.7 V and 1.7 V are observed on the first discharge curve which can be ascribed to an insertion reaction and a conversion reaction respectively according to the previous report [15]. A reversible capacity as high as 300 mAh g^{-1} is obtained at the first cycle, but decreases to 175 mAh g^{-1} immediately at the second

cycle. And after a complete activation at the third cycle, a reversible capacity of 145 mAh g^{-1} is maintained throughout the rest cycles. The charge and discharge characteristics indicate that the prepared cathode undergoes a typical conversion reaction [2].

The cycling stability of the prepared electrodes is also characterized and the results are presented in Fig. 5(b). After 100 cycles, large retentive capacities of 130 mAh g^{-1} at 14 mA g^{-1} and of 118 mAh g^{-1} at 71 mA g^{-1} are achieved, corresponding to 89.6% and 92% of the capacities at the third discharge process, respectively, demonstrating excellent cycling stability of the prepared electrode.

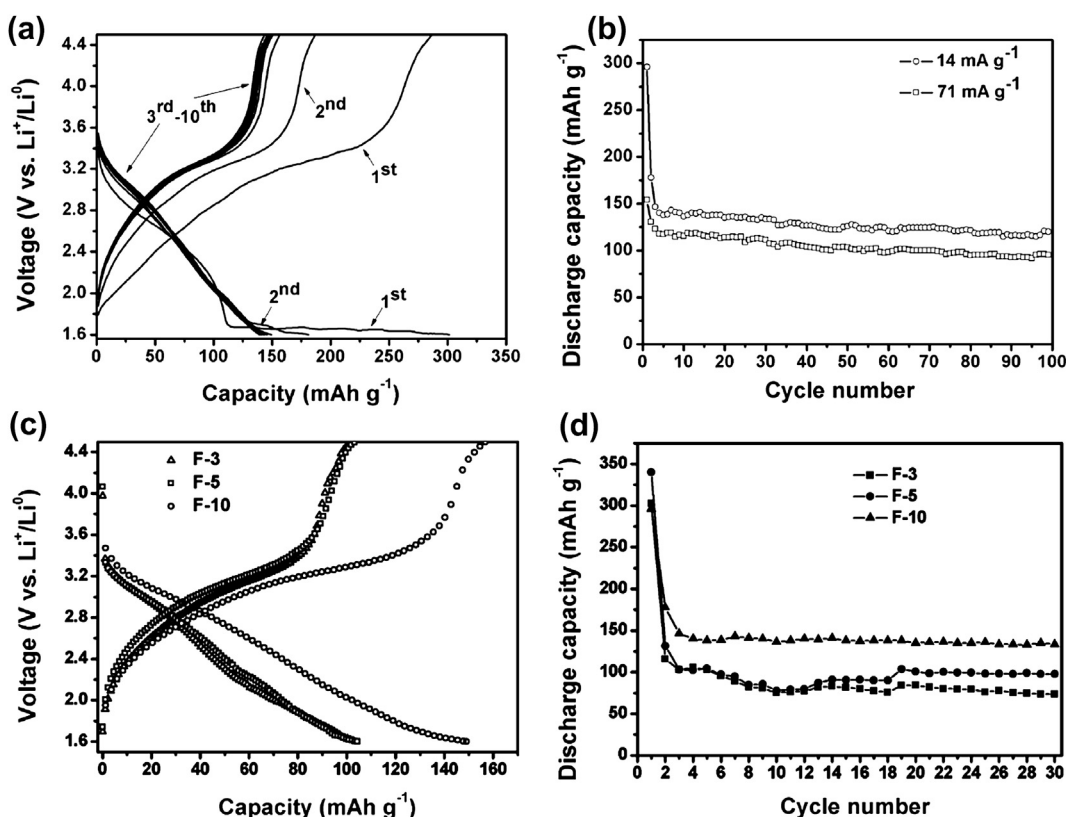


Fig. 5. (a) Charge–discharge curves of F-10 sample electrode for the first ten cycles with a current density of 14 mA g^{-1} , (b) Discharge capacity as a function of cycle number for F-10 sample electrode at different current densities between voltage range of $1.6\text{--}4.5 \text{ V}$ at 25°C , (c) the fifth charge–discharge curves after activation of F-3 (hollow triangle), F-5 (hollow square) and F-10 (Hollow circle) electrodes with a current density of 14 mA g^{-1} , (d) Discharge capacity as a function of cycle number for F-3 (solid square), F-5 (solid circle) and F-10 (solid triangle) electrodes with a current density of 14 mA g^{-1} between voltage range of $1.6\text{--}4.5 \text{ V}$ at 25°C .

Moreover, with the current density increasing from 14 mA g⁻¹ to 71 mA g⁻¹, a small capacity loss only of about 20 mAh g⁻¹ is observed and this value doesn't grow throughout the 100 cycles, which indicates the electrode having a good rate performance.

By comparison, the electrochemical behaviors of F-1, F-3 and F-5 should be measured. However, the electrochemical test of F-1 is hard to be carried out due to the production of F-1 is minimal. In this way, a comparison of the electrochemical performances of F-3, F-5 and F-10 is made to investigate the effect of the morphology on the electrochemical performances of the Fe_{1.9}F_{4.75}·0.95H₂O cathodes. As Fig. 5(c) indicated, F-10 shows a higher discharge plateaus and a lower charge plateaus, showing a better polarization performance compared with F-3 and F-5 cathodes. Simultaneously, its cycle performance is also much better than F-3 and F-5 cathodes with high stability and a much larger retentive capacity of 134 mAh g⁻¹ (98 mAh g⁻¹ for the F-5 cathode and 74 mAh g⁻¹ for the F-3 cathode) after 30 cycles at a current density of 14 mA g⁻¹ (Fig. 5(d)). The results show that the electrochemical behaviors of the Fe_{1.9}F_{4.75}·0.95H₂O cathodes are significantly influenced by the morphologies. And the main reason that the F-10 cathode possesses better polarization performance, excellent cycling stability and good rate performance might be ascribed to its worm-like mesoporous structure, which can accommodate a volume change during the cycle of the rechargeable lithium batteries under various current densities as analyzed previously.

4. Conclusion

In summary, by tuning the amount of ionic liquid used in fabrication, nanostructured iron-based fluorides with different morphologies are obtained, one of which with worm-like mesoporous structure shows promising cathode performances of rechargeable lithium ion batteries with a high discharge plateau around 2.7 V at the first cycle, a large reversible discharge capacity (as high as 145 mAh g⁻¹ at a current density of 14 mA g⁻¹), and an excellent rate performance with a small capacity loss of 20 mAh g⁻¹ even at the high current density of 71 mA g⁻¹ throughout 100 cycles. The satisfactory behaviors are ascribed to the high specific surface and the accommodation of the volume changes of the electrode benefited from the worm-like mesoporous structure. Therefore, it is believed that the electrochemical performance of fluoride cathodes can be further improved by varying synthesis conditions to

optimize the morphology and nanostructure of the iron-based fluorides in the future.

Acknowledgment

This work was financially supported by NSFC Project No. 50973127, research projects of Chinese Science and Technology Ministry No. 2007CB209700, and research projects from the Science and Technology Commission of Shanghai Municipality No. 08DZ2210900.

References

- [1] S. Okada, M. Ueno, Y. Uebou, J. Yamaki, *J. Power Sources* 146 (2005) 565–569.
- [2] J. Cabana, L. Monconduit, D. Larcher, M. Rosa Palacín, *Adv. Mater.* 22 (2010) E170–E192.
- [3] M.R. Palacín, *Chem. Soc. Rev.* 38 (2009) 2565–2575.
- [4] M. Nishijima, I.D. Gocheva, S. Okada, T. Doi, J. Yamaki, T. Nishida, *J. Power Sources* 190 (2009) 558–562.
- [5] N. Yabuuchi, M. Sugano, Y. Yamakawa, I. Nakai, K. Sakamoto, H. Muramatsu, S. Komaba, *J. Mater. Chem.* 21 (2011) 10035–10041.
- [6] Y. Makimura, A. Rougier, L. Laffont, M. Womes, J.C. Jumas, J.B. Leriche, J.M. Tarascon, *Electrochim. Commun.* 8 (2006) 1769–1774.
- [7] S.W. Kim, D.H. Seo, H. Gwon, J. Kim, K. Kang, *Adv. Mater.* 22 (2010) 5260–5264.
- [8] C. Li, L. Gu, S. Tsukimoto, P.A. van Aken, J. Maier, *Adv. Mater.* 22 (2010) 3650–3654.
- [9] C. Li, L. Gu, J. Tong, S. Tsukimoto, J. Maier, *Adv. Funct. Mater.* 21 (2011) 1391–1397.
- [10] D.S. Jacob, L. Bitton, J. Grinblat, I. Felner, Y. Koltypin, A. Gedanken, *Chem. Mater.* 18 (2006) 3162–3168.
- [11] Y.J. Zhu, W.W. Wang, R.J. Qi, X.L. Hu, *Angew. Chem. Int. Ed.* 43 (2004) 1410–1414.
- [12] G.S. Fonseca, A.P. Umpierre, P.F.P. Fichtner, S.R. Teixeira, J. Dupont, *Chem. Eur. J.* 9 (2003) 3263–3269.
- [13] D. Fox, J. Gilman, H. De Long, P. Trulove, *J. Chem. Thermodyn.* 37 (2005) 900–905.
- [14] R. Gillespie, J. Hartman, *Can. J. Chem.* 45 (1967) 859–863.
- [15] N. Yamakawa, M. Jiang, B. Key, C.P. Grey, *J. Am. Chem. Soc.* 131 (2009) 10525–10536.
- [16] R. Gedyne, F. Smith, K. Westaway, A. Humera, L. Baldisera, L. Laberge, et al., *Tetrahedron Lett.* 27 (1986) 279–282.
- [17] R.J. Giguere, T.L. Bray, S.M. Duncan, G. Majetich, *Tetrahedron Lett.* 27 (1986) 4945–4948.
- [18] M. Tsuji, M. Hashimoto, Y. Nishizawa, M. Kubokawa, T. Tsuji, *Chem. Eur. J.* 11 (2005) 440–452.
- [19] K. Ding, Z. Miao, Z. Liu, Z. Zhang, B. Han, G. An, S. Miao, Y. Xie, *J. Am. Chem. Soc.* 129 (2007) 6362–6363.
- [20] Y. Jiang, Y.J. Zhu, *J. Phys. Chem. B* 109 (2005) 4361–4364.